nating control female mice there were no untoward effects as judged by litter size, nearly identical birth weights, and weights of offspring at 30 days of age (Table 1). Offspring of MSG-treated females were significantly heavier at 30 days of age (Table 1). This was most likely the result of the reduced litter size seen in the MSG-treated females, which in turn allowed for increased availability of mother's milk. These weight differences were not observed in the male reproduction series (Table 1) when litter size is comparable.

The occurrence of reproductive dysfunction in both the female and male mouse along with reduced endocrine gland weights leads us to suspect that MSG administered during the neonatal period results in hypothalamic damage leading to multiple endocrine dysfunction. The multiple endocrine dysfunction hypothesis would account for a number of the behavioral observations made by us and other investigators. Stunted skeletal growth and obesity may result from disturbance of growth hormone (GH) production and release. Our obese animals consistently show abnormally large deposits of fatty tissue in the peritoneal cavity on autopsy. The role of GH in the mobilization of nonesterified fatty acids from fat deposits may, in part, account for the obesity of MSG-treated mice. The consistently reduced thyroid weights recorded above indicate a reduced secretion of thyroid-stimulating hormone which again suggests hypothalamic damage. Thyroid dysfunction may also account for the reduced activity that we observed and the decreased oxygen consumption reported by Djazayery et al. (11), indicating a much reduced metabolic rate. Early thyroid dysfunction may also affect CNS growth and development resulting in learning deficits. Finally, damage to the hypothalamus can result in decreased secretions of gonadotrophins necessary for female and male reproduction.

The delayed puberty seen in this study, indicated by delayed vaginal openings, is probably the result of a decreased estrogen output, since vaginal opening occurs as the result of an initial release of large amounts of ovarian estrogen. This suggests a delay in the initial release of gonadotrophin necessary for ovarian stimulation. The longer estrous cycles, decreased incidence of proestrus, and decreased ovarian weights indicate that gonadotrophin release is also impaired after puberty. These conclusions are supported by others who have noted irregularities in the estrous cycle and reduction in pituitary prolactin

and mammary gland development (3), along with a decrease in pituitary luteinizing hormone (12). A study on golden hamsters, in which the doses of MSG were higher than those we used, showed females to be acyclic with small follicles and no corpora lutea, while males had atrophic seminiferous tubules and reduced spermatogenesis (13). Thus, the reduced female fertility observed here may be due to either a decreased incidence of ovulation or a failure of implantation—events which are dependent on luteinizing hormone and prolactin. The decreased number of pregnancies from matings of control females and MSG-treated males is probably due to decreased spermatogenesis.

WILLIAM J. PIZZI
JUNE E. BARNHART
Department of Psychology,
Northeastern Illinois University,
Chicago, Illinois 60625
DON J. FANSLOW
Department of Biology,
Northeastern Illinois University

References and Notes

1. J. W. Olney, Science 164, 719 (1969).
2. ——, L. G. Sharpe, R. D. Feigin, J. Neuropathol. Exp. Neurol. 31, 464 (1972); N. Lemkey-Johnston and W. A. Reynolds, ibid. 33, 74 (1974).
3. H. Nagasawa, R. Yanai, S. Kikuyama, Acta Endocrinol. 75, 249 (1974).
4. S. N. Pradhan and J. F. Lynch, Jr., Arch. Int. Pharmacodyn. Ther. 197, 301 (1972); H. K. Berry, R. E. Butcher, L. A. Elliott, R. L. Brunner, Devel. Psychobiol. 1, 165 (1974).
5. P. E. Araujo and J. Mayer, Am. J. Physiol. 225, 764 (1973).
6. W. J. Pizzi and J. E. Barnhart, Pharmacol. Biochem. Behav. 5, 551 (1976).
7. W. A. Reynolds, A. S. Bingel, N. Lemkey-Johnston, Society for Gynecological Investigation, 19th meeting (1972), abstr., p. 46.
8. N. J. Adamo and A. Ratner, Science 169, 673 (1970).
9. G. P. Trentini, A. Botticelli, C. S. Botticelli, Fertil. Steril. 25, 478 (1974).
10. A. M. Potts, K. W. Modrell, C. Kingsbury, Am. J. Ophthalmol. 50, 900 (1960).
11. A. Djazayery, D. S. Miller, M. J. Stock, Proc. Nutr. Soc. 32, 31a (1973).
12. T. W. Redding, A. V. Schally, A. Arimura, J. Wakabayashi, Neuroendocrinology 8, 245 (1971).
13. A. Lamperti and G. Blaha, Biol. Reprod. 14, 362 (1976).
14. This work was supported by a grant from the Committee on Organized Research, Northeastern Illinois University, Chicago. We thank Cathy Genovese and Ruth Cisar for technical assistance.

23 June 1976; revised 29 November 1976

Chromatic Organization of Primate Cones

Abstract. The distributions of baboon retinal cones were mapped histochemically by light-stimulated reduction of nitroblue tetrazolium chloride. Blue cones were distributed regularly in the periphery; red and green cones were distributed randomly everywhere. The ordering of cone densities was green > red > blue.

Delineating the retinal circuits that channel and process chromatic information requires knowing the spectral classes of cone photoreceptors and how they are organized into a two-dimensional sensor matrix. The spectral types of goldfish cones have been classified by their morphologies and mosaic organization (1–3) with precision sufficient to permit the morphological analysis of color-specific contacts by some second-order neurons (4). Since all primate cones are morphologically identical according to present criteria, a comparable analysis of color-specific connections in primates has not been possible. Psychophysical data concerning the spatial properties of primate color processing are available, and large samples of spiking retinal and brain neurons with inputs from cones are being accumulated. Knowing the proportions and densities of cone types at various retinal loci might reveal how the cone mosaic relates to psychophysical performance and neural organization.

Microspectrophotometry has yielded evidence for three spectral types of primate cones (5), each containing a single visual pigment. We shall refer to these as red ($\lambda_{max} \cong 575$ nm), green ($\lambda_{max} \cong 535$ nm), and blue ($\lambda_{max} \cong 440$ nm) cones. By using histochemical techniques that we used to analyze the color organization of goldfish cones (1), we have been able to describe how red, green, and blue baboon cones are distributed.

When cones are bleached by light, they undergo temporary increases in the rate of mitochondrial electron transport, such increases being measurable as increased rates of reduction of nitroblue tetrazolium chloride (NBT) to a blue-violet product (NBT-diformazan) in the ellipsoids of stimulated cones (1, 2, 6). Eyes were enucleated under Nembutal anesthesia from dark-adapted (7) baboons (Papio cynocephalus) in dim light, opened with a semicircular cut below the corneoscleral junction, placed cut-side down on a pad saturated with iced Locke's saline inside an oxygenated lightproof cannister, and further dark-adapted for 30 minutes. Retinas were removed in infrared light ($\lambda > 800$ nm) through the use of infrared image converters and were mounted receptor-side up on a wax support. The retinas were moistened with Locks's saline (room temperature), oxygenated, and stimulated for 5 minutes with white light ($>10^7$

photon sec^{-1} μm^{-2} over 400 to 700 nm) or narrow-band spectral light from a monochromator (Bausch and Lomb; 5-nm bandpass at half-peak height) at 440, 555, or 650 nm. The retinas were then incubated for 10 minutes in a saline-succinate-NBT medium (8), fixed and mounted in 10 percent formalin–isosmotic phosphate buffer (pH 7.4), and examined as whole mounts. Since the spectral absorbances of cone pigments overlap, we examined histograms (9) of cone response magnitude (the amount of NBT reduced in response to a stimulus) in order to determine the stimulus flux densities at which the responses of a single population of cones were sufficiently isolated.

Virtually all cones stimulated with white light responded strongly (Fig. 1a). At eccentricities of 5° to 40° (10), blue lights (440 nm) elicited responses in 12 to 14 ($\bar{X} = 13.4$) percent of the cones, and the cones were regularly arrayed (11) (Fig. 1b). Two experiments at 5.1 × 10⁴ and one each at 4.0 × 10⁴ and 8.0 × 10⁴ photon sec^{-1} μm^{-2} yielded identical results. Red lights (650 nm, 2.6 × 10⁵ photon sec^{-1} μm^{-2}) elicited responses in 30 to 34 percent of the cone population ($\bar{X} = 33.0$) (Fig. 1c) in areas sampled at eccentricities of 8° to 40°. This proportion was confirmed with response histogram data (9) as representing the isolated red cone population. According to statistical criteria, the red cones were randomly distributed. The spectral absorbances of red and green cone pigments overlap to such a degree that it was not possible to isolate green cone responses. Stimulating with 555-nm lights (5.0 × 10⁵ and 1.1 × 10⁶ photon sec^{-1} μm^{-2}) elicited responses in 88 percent of the cones, and the unresponsive cones (12 percent) were arrayed in a regular pattern. This would be the expected result if the 555-nm light stimulated red and green cones but did not stimulate blue cones. From these experiments we conclude the cone proportions at eccentricities greater than 5° to be 13 percent blue cones, 54 percent green cones, and 33 percent red cones.

Responses of blue cones were studied throughout the central 2° in three foveas (12) with 440-nm light (two experiments at 8.0 × 10⁴ and one at 3.0 × 10⁴ photon sec^{-1} μm^{-2}). Between the foveola and about 0.25° and 0.5°, only 3 to 4 ($\bar{X} = 3.1$) percent of the cones responded (Fig. 1d). The distribution appeared somewhat patterned but was statistically random according to our tests. The proportion of blue cones increased to 20 percent at 1°. At 5°, the proportion of blue cones was down to 12 to 14 percent. One successful foveal red-light experiment

(650 nm, 1.0 × 10⁵ photon sec^{-1} μm^{-2}) indicated that red cones probably represented between 30 and 40 percent of the cones in the foveola. A more accurate estimation was precluded as a result of mechanical distortion and poor fixation of the tissue.

Knowing the proportions of cone types at several retinal loci permits us to estimate cone density functions for each type by partitioning the total cone density function of the baboon retina according to the proportions of red, green, and blue cones (assuming that the changes in proportions between our discrete measurements are smooth, contin-

uous functions and that red cones constitute 33 percent of the cones everywhere in the retina). The blue cone density is maximal at about 1°, and the red and green cone densities are maximal in the foveola (Fig. 2). These results coincide with the loci of the psychophysically determined maxima in the increment threshold sensitivities of the isolated human blue, green, and red mechanisms (13, 14).

Most of the ganglion cells in the fovea of the rhesus monkey have concentrically organized receptive fields, the centers of which receive inputs from one spectral class of cones, while the an-
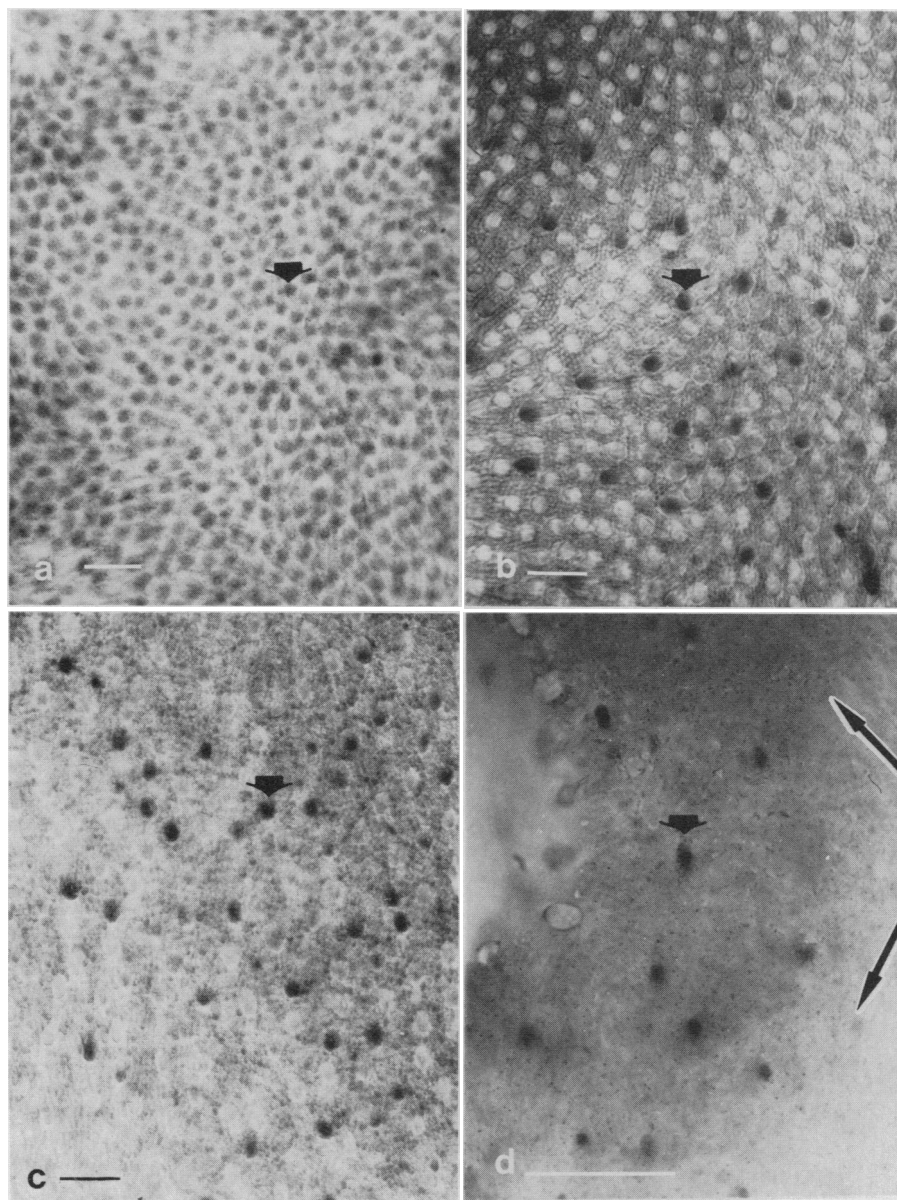

Fig. 1. Flat mounts of baboon retinas after stimulation with light and incubation with NBT. All scale markers indicate 25 μm. Wide arrows indicate cone ellipsoids containing NBT-diformazan. (a) White light exposure, >10⁷ photon sec^{-1} μm^{-2} across 400 to 700 nm, 10° temporal retina. Two percent of the cones failed to respond. (b) Blue light exposure, 5.1 × 10⁴ photon sec^{-1} μm^{-2}, 440 nm, 25° temporal retina. (c) Red light exposure, 2.6 × 10⁵ photon sec^{-1} μm^{-2}, 650 nm, 40° temporal retina. (d) Blue light exposure, 8.0 × 10⁴ photon sec^{-1} μm^{-2}, 440 nm, foveola. Retina is torn at upper left; thin arrows indicate positions of two responsive cones that are out of focus.

Fig. 2. Estimated density distributions for red (R), green (G), and blue (B) cones, constructed by partitioning the total cone density function for temporal retina (T) according to the relative proportions of red, green, and blue cones in the various retinal areas described. We assumed that the transition between regions containing differing proportions of a given cone type, as determined by discrete measurements, was a smooth, continuous function and that red cones represented 33 percent of the cones at all loci. (Inset) Expanded blue (B) cone density function. Dashed line indicates change of scale on the abscissa.

Eccentricity (Degrees of arc)
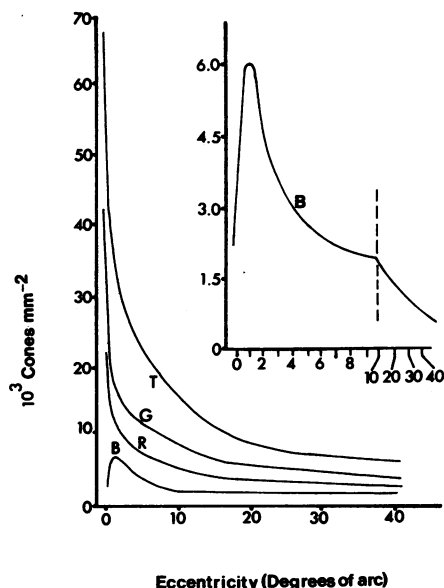
tagonistic surrounds receive inputs from other classes (15). These cells are referred to as color-opponent ganglion cells. In the rhesus monkey, the frequency of encountering such ganglion cells with blue-sensitive receptive field centers is 3 percent for 0° to 0.5°, 16 percent for 0.5° to 2°, and 11 percent for 2° to 10° [calculated from the data of De Monasterio and Gouras (15)]. In our baboons, the proportions of blue cones are 3, 20, and 13 percent for the same retinal areas. In the baboon foveola the mean intercone distance of 6 ± 0.59 minutes of arc (uncorrected for shrinkage) for blue cones is close to the psychophysically determined value of 6.5 to 7.5 minutes of arc for the acuity of the human blue mechanism (13, 16). Our single observation that red cones are less frequent than green cones in the foveola is consistent with the spectral acuity data of Brindley (13) and the contrast sensitivity data of Kelly (17), which indicate that green cones are more densely packed than red cones in the fovea. Also, in the rhesus monkey (15), color-opponent ganglion cells with green-sensitive receptive field centers are encountered twice as frequently between 0° and 0.5° as red-center cells of the same class. It appears that the ordering of cone densities (green > red > blue) holds true over the entire retina and may be reflect-

ed in certain neuronal populations as well.

The major consequences of these results are that (i) a basis now exists for estimating the numbers of red, green, or blue cones in the receptive fields of visual neurons, and (ii) the arrangements of dendritic contacts of certain retinal neurons may reflect the distributions of red, green, or blue cones.

ROBERT E. MARC
Jules Stein Eye Institute, University of
California, Los Angeles 90024
HARRY G. SPERLING
Graduate School of Biomedical
Sciences, University of Texas
Health Science Center,
Houston 77025

References and Notes

1. R. E. Marc and H. G. Sperling, Science 191, 487 (1976).
2. _____, Vision Res. 16, 1211 (1976).
3. W. K. Stell and F. I. Hárosi, ibid., p. 647.
4. W. K. Stell, J. Comp. Neurol. 159, 503 (1975); _____ and D. O. Lightfoot, ibid., p. 473; _____, T. G. Wheeler, H. F. Leeper, Science 190, 989 (1975).
5. W. B. Marks, W. H. Dobelle, E. F. MacNichol, Jr., Science 143, 1181 (1964); P. K. Brown and G. Wald, ibid. 144, 45 (1964); P. A. Liebman, in Handbook of Sensory Physiology, vol. 7, part 1, Photochemistry of Vision, H. J. A. Dartnall, Ed. (Springer-Verlag, Berlin, 1972), pp. 481–528.
6. J. M. Enoch, Invest. Ophthalmol. 2, 16 (1963).
7. In a few experiments animals were obtained from other investigators at the terminations of preparations conducted in room light. The eyes were immediately enucleated, cut open, and sealed in the dark, oxygenated cannister.
8. Incubation medium stock solution: 35 percent (by volume) disodium-monosodium phosphate buffer (97 mM, pH 7.4), 35 percent Locke's saline, 30 percent disodium succinate solution (100 mM). Before each experiment, 5 mg of NBT (Sigma) was dissolved in 1 ml of stock solution. The final pH was 7.4.
9. A response histogram is a plot of the number of cones showing a certain magnitude of "response" (measured microspectrophotometrically in individual cone ellipsoids as the absorbance of NBT-diformazan at 570 nm) versus the range of possible response magnitudes. By constructing such histograms for experiments at several flux densities and wavelengths of stimulation, it is feasible to determine when a population of cones has been isolated (2).
10. Conversion of linear distance to visual angle was made by assuming the baboon eye to be optically equivalent to the rhesus monkey eye as described by E. T. Rolls and A. Cowey [Exp. Brain Res. 10, 298 (1970)]. This assumption is supported by our observation that the eyes of the two species are anatomically similar with respect to globe size, cone density versus eccentricity curves, the distance between the foveola and the optic disk, and the distribution of macular pigment (M. L. J. Crawford and R. E. Marc, unpublished data).
11. Regularity of patterning was evaluated by a χ^2 test of the goodness of fit between observed distributions of intercone distances or numbers of quadrats of a given density and those predicted by a Poisson distribution (random dispersal of spatial elements) [R. C. McLean and W. R. Ivimey-Cook, Textbook of Theoretical Botany (Longman, London, 1973), vol 4, pp. 3457–3470]. Peripheral blue cones were regularly patterned ($P < .001$); all other distributions were random ($P > .05$).
12. Two-thirds of our foveal preparations were unsuccessful for two major reasons: (i) tearing of the fovea during isolation under infrared light and (ii) retinal respiratory failure.
13. G. S. Brindley, J. Physiol. (London) 124, 400 (1954).
14. G. Wald, J. Opt. Soc. Am. 57, 1289 (1967).
15. F. M. De Monasterio and P. Gouras, J. Physiol. (London) 251, 167 (1975); _____, D. J. Tolhurst, ibid., pp. 197 and 217.
16. D. C. West, Vision Res. 7, 949 (1967); N. W. Daw and J. M. Enoch, ibid. 13, 1669 (1973); J. Pokorny, C. H. Graham, R. N. Lanson, J. Opt. Soc. Am. 58, 1410 (1968).
17. D. H. Kelly, J. Physiol. (London) 228, 55 (1973).
18. Supported in part by NSF grant BNS76-07854, NIH grant EY-00381, and grant FD-00687 from the Food and Drug Administration. We thank P. Pollack, N. Ishihara, Y. Miyakawa, and H. Naritomi for specimens; M. L. J. Crawford for technical assistance; and W. K. Stell, H. F. Leeper, A. Ishida, and D. Marshak for discussion.

4 October 1976; revised 16 November 1976